Effects of Natural Gas–Hydrogen–Oxygen Blends on Combustion Behavior and NO_X Formation in Industrial Burners

Osman Kumuk [a], Isabel Amez [b,c], Bugrahan Alabas [d*]

a. Unmanned Aerial Vehicle Technology and Operatorship Program, Iskenderun Vocational School of Higher Education, Iskenderun Technical University, Hatay, Turkiye
b. E.T.S. Ingenieros de Minas y Energía, Universidad Politécnica de Madrid, Madrid, Spain
c. Laboratorio Oficial J.M. Madariaga (LOM)- TECMINERGY, Getafe, Madrid, Spain
d. Department of Aeronautical Engineering, Faculty of Aeronautics and Astronautics, Erciyes University, Kayseri, Turkiye

* Corresponding author: bugrahanalabas@erciyes.edu.tr

Keywords

Natural Gas;
Hydrogen;
Oxygen Enrichment;
Combustion;
NO_X;

Abstract

Hydrogen gas plays a crucial role as a fuel in renewable energy projects. Water electrolysis is used when hydrogen gas is produced through renewable and green methods. This method, however, remains open to development due to its high cost. Oxygen is also produced along with hydrogen gas during water electrolysis. This study proposes that, to reduce the cost of hydrogen production, the oxygen generated during production should be directly burned in a nearby burner without any storage. For this purpose, hydrogen gas was added to natural gas at volumetric rates of 10%, 20%, and 30% in a burner maintained at a constant thermal power of 33 kW. Furthermore, the oxygen-enriched combustion method was applied to all natural gas/hydrogen mixtures. The results show that hydrogen addition increases the combustion chamber exit temperature. Furthermore, during the oxygen enrichment process, both flame temperature and boiler exit temperature increased up to 31% O_2. After this O_2 level, the temperature values decreased. Furthermore, NO_X emissions at the combustion chamber exit showed a linear change with temperature data. Especially at high Hydrogen ratios, NOX emissions of 28.5% O_2 and above 20 ppm were detected.

Highlights

- Direct use of electrolytic H_2 and O_2 in an industrial burner was experimentally evaluated.
- Increasing H_2 fraction in CH_4 raised combustion chamber exit temperatures.
- O_2 enrichment improved flame temperature up to 31% O_2, after which instabilities reduced temperatures.
- High O_2 levels caused intense near-burner combustion and rapid downstream temperature drop.
- NO_X emissions increased linearly with temperature and exceeded 20 ppm at high H_2 and ≥28.5% O_2.
- Optimal performance was achieved with 70% CH_4–30% H_2 and 26.1% O_2 in the combustion air.
- Using electrolytic O_2 directly in combustion can enhance the cost-effectiveness of green H_2 production.

1. Introduction

Hydrogen energy holds promise in many areas, including land transportation, aviation, home heating, and electricity generation. Researchers are conducting intensive studies to utilize hydrogen energy more efficiently in industrial applications. Currently, the most commonly used fossil fuels contain high amounts of carbon atoms. These atoms undergo an exothermic reaction with oxygen in the air, producing CO_2. On the other hand, hydrogen atoms, when they undergo combustion, only produce H_2O (water) [1]. Because it does not produce any carbon-containing emissions as a result of energy production, hydrogen is considered a fuel of the future in zero-emission studies. However, significant challenges remain in the transition to hydrogen energy. Hydrogen does not exist alone as a fuel in nature; it can be produced from fossil fuels to make it a combustible fuel. Alternatively, it can be produced cleanly through the electrolysis of water [2]. The method of using electricity generated from clean and renewable sources, such as solar or wind, during hydrogen production is called green hydrogen production. Although this method results in zero emissions, it is very costly. The energy required to electrolyze water is higher than the energy generated by the combustion of hydrogen, which recombines with oxygen. For this reason, many researchers have criticized hydrogen energy.

When energy is generated through renewable sources such as solar and wind, this energy is directly converted into electricity and fed into the grid. Conversely, when demand in the electricity grid is low, excess energy generated can unbalance the grid. One of the optimal methods for green hydrogen production is to direct excess energy from solar and wind energy to hydrogen production [3]. In this production method, hydrogen is produced as a result of the electrolysis of water. Storing or transporting the produced hydrogen to its intended use creates additional problems and costs. As a solution to this problem, transporting a natural gas/hydrogen mixture in existing natural gas (NG) lines is being tested in some European countries. These studies indicate that up to 20% volumetric hydrogen can be transported in a mixture with natural gas. No design changes are required in existing natural gas lines for this transportation [4]. Another component produced during the electrolysis of water to produce hydrogen is oxygen. This high-purity oxygen is used in fields such as steel and metallurgy, including the healthcare sector. Furthermore, studies are also being conducted on applications where this oxygen is used directly for combustion. Amez et al. [5] proposed the

method shown in Figure 1 in their study. According to this system, the hydrogen and oxygen gases produced during green hydrogen production are burned directly in a natural gas burner rather than being stored or transported. The study determined the optimum data required for electrolysis. Furthermore, an oxygen enrichment process was applied to pure methane in an industrial burner, and combustion chamber exit temperature and emissions were obtained. This study discusses the benefits of oxygen enrichment in an industrial burner on combustion efficiency and its compatibility with electrolysis optimization.

Studies on hydrogen-enriched combustion of methane flames have a significant and current place in the literature, both experimentally and numerically. These studies have tested different burner types and investigated different combustion methods. Al Bishtawi et al. [6] investigated the effect of hydrogen addition to a methane-air flame on flame development. In the numerical study, the unburned mixture temperature increased as the hydrogen content in the fuel increased. Furthermore, an increase in the hydrogen content decreased the stand-off distance. Alsharif and Woolley [7] investigated the effects of equivalence ratio and hydrogen addition on methane and propane flames in a vertical tube burner. In this study, they suggested that velocity coupling is the primary mechanism causing acoustic instability. The highest combustion velocity in methane flames occurred at $\phi = 1.1$. Bayramoglu et al. [8] studied the emissions and performance of hydrogen-enriched methane combustion. The steam methane reformer method used in hydrogen production was investigated in the study. According to the highest and lowest reformer inlet speeds, 40% hydrogen production was achieved. This significantly reduced CO_2 emissions. Zhao et al. [9] numerically investigated the pollutant emissions of methane/hydrogen combustion under porous media burner conditions. The results showed that when the hydrogen addition ratio was increased to 40%, NO_X emissions increased by up to 4.25 times. CO emissions decreased with increasing inlet air temperature. Increasing the combustion pressure reduced both CO and NO_X emissions. Xu et al. [10] investigated the formation of NO emissions from a hydrogen-enriched methane flame in a swirl burner. The results showed that the main NO production mechanism in swirl combustion occurs via thermal pathways. The majority of NO emissions occurred in the high-temperature region at the burner outlet.

Hydrogen enrichment of natural gas has attracted considerable attention due to several favorable combustion characteristics. Compared with conventional methane combustion, hydrogen addition increases the laminar burning velocity, reduces ignition delay time, extends lean flammability limits, and improves flame stability. These characteristics contribute to enhanced combustion efficiency and more reliable operation under lean conditions. Furthermore, hydrogen-enriched combustion can facilitate lower carbon emissions by partially replacing carbon-containing fuels with a carbon-free energy carrier. When hydrogen and oxygen produced simultaneously through water electrolysis are directly utilized in combustion systems, additional benefits can be achieved through improved energy utilization and reduced greenhouse gas emissions. Previous studies have demonstrated that methane–hydrogen mixtures provide superior combustion performance and enhanced flame propagation characteristics, making them promising candidates for future low-carbon combustion technologies [11–13].

Many studies in the literature show that hydrogen is used not only in mixture with methane but also with different fuels such as kerosene, ammonia, and biogas [14]. In addition to all these studies, there are also studies examining the effects of changing the O_2 and N_2 ratios in the combustion air on combustion and emission performance. Among these studies, the method in which the oxygen ratio in the combustion air is increased is called oxygen-enriched combustion. Oxygen enrichment can be applied to different fuel mixtures as well as to fuels containing hydrogen, according to the literature. Guo et al. [15] tested the combustion of premixed ammonia enriched with hydrogen and oxygen. The results showed that oxygen enrichment improved the ignition properties. As the oxygen ratio increased, the combustion duration initially decreased and then increased. Mutlu and Taştan used propane as a hydrocarbon in their study. They examined flame characteristics and emission values by applying different rates of O_2 enrichment to a propane flame. The results show that as the O_2 content in the combustion air increases, CO emissions decrease while NO_X emissions increase. An et al. [16] investigated the flame stability and emission behavior of oxygen-enriched ammonia combustion in a swirl combustor. The results showed that when the O_2 ratio was increased from 21% to 35%, the NO mass fraction increased by a factor of six. Furthermore, as the O_2 ratio exceeds 30%, the fuel NO mechanism becomes more dominant. Tunç [17] investigated the oxygen enrichment performance of a methane/hydrogen mixture from a thermoacoustic perspective. In the study, 20% hydrogen was added to the methane flame by volume. The results showed that a high oxygen ratio resulted in a higher flame temperature. Furthermore, the change in the swirl number produced a 3% temperature increase.

A review of the literature reveals that methane flame enrichment with hydrogen has been studied to achieve low emission targets. These studies tested various alternative fuels, as well as different burners and combustion conditions. The oxygen enrichment method has become quite popular as an innovative combustion technology in recent years. The majority of these studies were conducted in model burners. The high combustion speed of both hydrogen and oxygen increases the tendency for flashback. Due to this hazard, studies using both oxygen and hydrogen in combination in industrial burners are rare. Amez et al. [5] used a Bentone BFG1 H3 brand burner in their experimental study. This study tested the use of oxygen generated during hydrogen production in an industrial burner and combustion chamber. Combustion chamber temperature values and pollutant emissions were determined. However, due to the high risk of flashback, the scenario in which hydrogen is also introduced into the burner under oxygen enrichment conditions was not experimentally tested. Furthermore, because the flame remained within the boiler in this study, flame formation and temperature could not be determined. Furthermore, the axial temperature distribution within the combustion chamber could not be investigated. This new research will numerically verify the reference study and investigate both hydrogen and oxygen enrichment. Unlike studies in the literature, a medium-sized burner with a maximum thermal power of 100 kW, suitable for industrial applications, will be used instead of a pilot burner. This numerical analysis will test a scenario in which hydrogen and oxygen produced by electrolysis are simultaneously fed to the burner, without high flashback and

explosion risks. This will allow flame temperature and formation, combustion chamber axial temperature distribution, and exit temperature to be determined. Furthermore, the formation and variation of NO_X emissions at the combustion chamber exit will be investigated. Thanks to this study, researchers will gain information about the effects of a situation where both Hydrogen and Oxygen can be increased simultaneously in industrial burners.

2. Materials and Methods (Methodology)

This section presents the geometric model and network structure of the numerical study. The flow rates and oxygen ratios of the fuel mixtures used in the study are also specified. The hydrogen and oxygen additions to the 100% natural gas flame are presented as input parameters for the study.

2.1. Numerical Model

In this study, the Bentone BFG1 H_3 brand burner, which Amez et al. [5] used experimentally, was taken as a reference. Figure 1 shows the burner mounted on the validated combustion chamber. The outer diameter of the cylindrical combustion chamber shown is 84 cm. Its length is 1 meter. There is a 14 cm diameter exhaust opening at the combustion chamber exit. On the other hand, the exit diameter of the burner mounted in the combustion chamber is 9 cm. The total burner length is 13 cm, of which 5 cm remains inside the combustion chamber in a barrel shape. The reference burner can operate at thermal power between 25 and 100 kW.

Figure 2 shows the three-dimensional geometric drawings and mesh structures of the combustion chamber and burner. A denser mesh was applied to the burner's outlet region to improve modeling accuracy. Table 1 shows the boundary and inlet conditions used in the numerical analyses. Commercially used burners utilize ambient air to create internal premixing, thus achieving combustion. Furthermore, like many commercial burners, they maintain combustion with a 20% excess air coefficient for low emissions. In this case, the equivalence ratio is calculated as 0.83.

In this study, in addition to the parameters held constant, there are also parameters whose changes are observed. These values are presented in Table 2 as a numerical analysis matrix. Three different fuel mixtures were analyzed, starting with 100% methane and ending with a mixture containing 30% H_2. Furthermore, all these fuel mixtures were analyzed at $O_2/N_2 + O_2$ ratios of 20.8%, 23.5%, 26.1%, 28.5%, 31%, and 33.9% by volume. Thus, the effects of both oxygen enrichment and hydrogen addition on the methane flame were investigated. Table 2 shows the fuel mixtures and the volumetric flow rates of methane and hydrogen required to provide this mixture. These flow rates were calculated based on 33 kW of thermal power. The lower heating values of all fuel mixtures by mass are also presented in the table. The lower heating values (LHV) of the fuel mixtures will be an important indicator when evaluating experimental data.

2.2. Governing equations

Transport equations for all species are continuity, energy, and momentum, and they were employed in computational fluid dynamics studies. The general form of the transport equation is shown in Eq. (1) [18,19].

$$\frac{\partial(\rho\phi_k)}{\partial_t} + \frac{\partial}{\partial x_i}\left(\rho u_i \phi_k - \Gamma_k \frac{\partial \phi_k}{\partial x_i}\right) = S_{\phi_k} \; k = 1, \ldots, N \tag{1}$$

Y_P is the mass fraction of any product species, P
Y_R is the mass fraction of a particular reactant, R
A is an empirical constant equal to 4.0
B is an empirical constant equal to 0.5
The net rate of production of species i due to reaction r, $R_{i,r}$, is given by the smaller (i.e., limiting value) of the two expressions below:

The Arrhenius reaction rate phrase:

$$R_{i,r} = \nu'_{ir} M_{w,i} A \rho \frac{\varepsilon}{k} \min_R \left(\frac{Y_R}{\nu'_{R,r} M_{w,R}}\right) \tag{2}$$

The reaction rate:

$$R_{i,r} = \nu'_{ir} M_{w,i} A B \rho \frac{\varepsilon}{k} \frac{\Sigma_P Y_P}{\Sigma_j^N \nu''_{j,r} M_{w,j}} \tag{3}$$

Eqs. (2)-(3) describe the chemical reaction rate, which is calculated using the large eddy mixing time scale k/ε, as defined in Spalding's eddy-dissipation model [20]. When the turbulence scale *k/ε>0*, combustion is sustained continuously without the need for an external ignition source.

NO_X formation mechanisms

The thermal NO_X formation mechanism is given in Eqs. (4)-(14) [19,21].

$$O + N_2 \leftrightarrow N + NO \tag{4}$$

$$N + O_2 \leftrightarrow O + NO \tag{5}$$

$$N + OH \leftrightarrow H + NO \tag{6}$$

$$k_{f,1} = 1.8\times10^{8} e^{-38370/T} \tag{7}$$

$$k_{f,2} = 1.8\times10^{4} T e^{-4680/T} \tag{8}$$

$$k_{f,3} = 7.1\times10^{7} e^{-450/T} \tag{9}$$

$$k_{r,1} = 3.8\times10^{7} e^{-425/T} \tag{10}$$

$$k_{r,2} = 3.81\times10^{3} T e^{-20820/T} \tag{11}$$

$$k_{r,3} = 1.7\times10^{8} e^{-24560/T} \tag{12}$$

$$\frac{d[NO]}{dt} = k_{f,1}[O][N_2] + k_{f,2}[N][O_2] + k_{f,3}[N][OH] - k_{r,1}[NO][N] - k_{r,2}[NO][O] - k_{r,3}[NO][H] \tag{13}$$

$$\frac{d[NO]}{dt} = 2k_{f,1}[O][N_2]\frac{\left(1-\frac{k_{r,1}k_{r,2}[NO]^2}{k_{f,1}[N_2]k_{f,2}[O_2]}\right)}{\left(1+\frac{k_{r,1}[NO]}{k_{f,2}[O_2]k_{f,3}[OH]}\right)}\left(mol/m^3-s\right) \tag{14}$$

The prompt NO_X formation mechanism is given in Eqs. (15)-(22) [19,21].

$$CH + N_2 \leftrightarrow HCN + N \tag{15}$$

$$N + O_2 \leftrightarrow O + NO \tag{16}$$

$$HCN + OH \leftrightarrow CN + H_2O \tag{17}$$

$$CN + O_2 \leftrightarrow NO + CO \tag{18}$$

$$CH_2 + N_2 \leftrightarrow HCN + NH \tag{19}$$

$$HCN + N \leftrightarrow N_2 + ... \tag{20}$$

$$\frac{d[NO]_{pr}}{dt} = fxAx\left(\frac{RT}{p}\right)^2[Fuel][O_2]^b[N_2]x\exp\left(\frac{E_a}{RT}\right) \tag{21}$$

$$S_{NO} = M_{NO}\frac{d[NO]}{dt} \tag{22}$$

The eddy-dissipation combustion model was chosen for the consumption of CH_4/H_2 mixed fuel. This model is commercially used due to its practicality. In this model, single-step global reactions are solved for the combustion of both hydrogen and methane. The single-step global reactions are as follows Eqs. (23)-(24):

$$CH_4 + 2O_2 = CO_2 + 2H_2O \tag{23}$$

$$2H_2 + O_2 = 2H_2O \tag{24}$$

3. Results and Discussion

The most fundamental and initial criterion for a numerical study is to verify data obtained experimentally from a reference model and accept it as accurate in the literature. After this verification, the impact of system modifications on the data can be investigated. In this study, the combustion chamber outlet temperature values in the reference study article [5] were verified. The data were taken from the flue section of the combustion chamber. The verified data are combustion chamber outlet temperature data. A similar decrease in combustion chamber outlet temperature was found after a 31% O_2 ratio in both experimental and numerical studies. Many studies in the literature show that oxygen enrichment increases temperatures in both the flame zone and other regions of the combustion chamber. However, there is a critical point for this increase for different fuel mixtures and combustors. After this point, a reverse effect can be observed. The key is to identify this critical point and to evaluate the data scientifically. All these changes will be analyzed under different H_2 addition conditions and compared with different applications in the literature.

Two important data points to be evaluated from the numerical results of the study are the combustion chamber exit temperature and the combustion chamber temperature distributions. Figure 3 shows a comparison of temperature data taken from the chimney at the combustion chamber exit. These data compare combustion analyses with air of varying O_2 contents for pure methane and hydrogen additions up to 30%. The analysis yielded consistent results for both hydrogen addition and increased oxygen content in the combustion air. The results show that increasing the hydrogen volume in the fuel mixture increases the flue gas exit temperature. Furthermore, this upward trend is more pronounced at higher O_2 ratios, such as 31% and 33.9%. Conversely, as the $O_2/N_2 + O_2$ ratios in the combustion air are increased, the flue gas exit temperatures increase steadily up to 31%. Temperatures reached 820 K at the highest hydrogen and 31% O_2 ratios. Average temperature increases of 100 K were observed for all fuel mixtures. Additionally, when the O_2 content was increased to 33.9% in all fuel blends, a further decrease in combustion chamber exit temperature was observed. To accurately interpret these data, data such as the maximum temperature within the combustion chamber, the temperature distribution, and the axial distance at which the maximum temperature occurs must also be explained.

Figure 4 shows the temperature changes in the combustion chamber as the axial distance from the burner center increases. Four different graphs are presented for different hydrogen ratios, and the most significant finding is the maximum temperature values. When all results are examined, the temperature values decrease as the axial distance from the burner exit to the chimney is increased. This is an expected result due to heat transfer through the boiler walls and the distance from the flame zone. When other results are examined, the flame exit temperature increases with the increase in oxygen content, similar to the chimney exit temperature. Furthermore, when the O_2 ratio was increased to 33.9%, the flame temperature decreased again at all H_2 ratios. When the maximum flame temperature is examined, the maximum temperature point remains between 0.1 and 0.15 m from the burner exit under standard air combustion conditions, while the maximum temperature point is moved 0.2 m beyond due to oxygen enrichment. Conversely, at higher oxygen ratios, a sudden drop occurs after the high temperatures, resulting in lower temperature data in the 0.3-meter region.

The exhaust gas temperature data used for model validation were obtained from the reference experimental study conducted by Amez et al. [5]. In that study, the temperature was measured by means of a thermocouple installed in the flue gas section located at the combustion chamber outlet. To ensure consistency, the numerical temperature values were extracted from the same outlet region of the combustion chamber. As shown in Figure 3, the numerical predictions are in good agreement with the experimental measurements, with only minor deviations observed at certain oxygen enrichment levels. These differences can be attributed to thermocouple measurement uncertainties, radiative heat exchange effects, wall heat losses in the experimental setup, and simplifications associated with the turbulence–chemistry interaction model employed in the CFD simulations. Despite these differences, the numerical model accurately reproduces the overall trend of exhaust gas temperature variation with increasing oxygen concentration.

While the O_2 atoms in the oxidizing air accelerate the combustion reaction, the N_2 atoms act as an inert gas, slowing the reaction and absorbing energy. Reducing the N_2 ratio in the oxidizing air increases the adiabatic flame temperature. Many studies in the literature have observed higher flame temperatures in combustion with high-oxygen air [22]. Reducing the entry of N_2 gas, which does not directly participate in the combustion reaction, into the combustion chamber also reduces the inert heat required to heat this gas. Conversely, reducing the N_2 in the air and increasing O_2 to high levels increases the laminar combustion speed above critical levels. The increased laminar combustion speed shortens the reaction residence time [23]. Therefore, the carbon and hydrogen atoms in the fuel do not have enough time to react with the oxygen atoms in the air. As a result, insufficient heat was released due to insufficiently reacting fuel and air, leading to a decrease in flame temperature. One of the most important indicators is that the flame temperature is more intense at the burner exit under high oxygen conditions. Flames with high laminar combustion speeds are observed to have shorter flame lengths. In flames containing N_2 or similar diluents in the air, the flame temperature is lower in the reaction zone at the burner exit. In contrast, temperatures may increase toward the outer flame region. Min et al. [24] investigated the effects of three different diluents: CO_2, Ar, and N_2. Flame length was observed to increase with the addition of all diluents. Alabaş et al. [25] observed in their experimental studies that temperatures decreased in thermocouples near the burner exit when N_2 and Ar were added, while a slight increase was observed at an axial distance of 15 cm from the burner exit. This suggests that the high concentration of N_2 slows down the reaction process, allowing the flame to spread over a wider area. Another result obtained in the study is that the increase in flue gas outlet temperature due to H_2 addition appears to be related to the increased lower calorific value. Although the thermal power remained constant, the higher mass calorific value

of H_2 gas increased the lower calorific value. While the lower calorific value of the fuel mixture under 100% methane combustion was 50,144 kJ/kg, it increased to 53,743 kJ/kg in the fuel mixture with 30% H_2 addition.

The discrepancies between numerical and experimental temperatures can be attributed to measurement uncertainties, heat losses in the experimental system, and simplifications inherent to the CFD model. Nevertheless, the numerical model accurately predicts the overall temperature trend and correctly identifies the critical oxygen concentration at which the exhaust gas temperature begins to decrease. At oxygen concentrations above 31%, the increased flame speed promotes localized heat release near the burner exit, resulting in shorter residence times and enhanced wall heat losses, which contribute to the observed reduction in exhaust gas temperature.

Figure 5 demonstrates the impact of H_2 molar concentration on axial temperature profiles across different O_2 %. As depicted in the figure, temperature ratios rapidly increased at the flame front due to the finely concentrated flame observed in all cases. After this point, temperatures significantly dropped beyond approximately between 15-20 cm from the burner on average 1300 K levels. For each study, it is clear that the flames advanced closer to the burner's exhaust with increasing hydrogen levels, a trend also visible in Figure 6. Regarding hydrogen addition, temperature values increased for all cases with a rise in reaction rate. Subsequently, a increased oxygen molar concentration within the combustor formed a broader, more volumetrically distributed flame.

Thermal field

Examination of Figure 7 reveals that the highest flame temperature levels slightly increased with the adding of hydrogen to the combustion chamber. Additionally, the flame position shifted further away with the increase in hydrogen concentration. As a result, with higher H_2 concentration, the H_2 flow rate increased, causing the flame position to move farther from the combustor. However, as the O_2 molar concentration decreased from 33.9 % to 20.8 %, the flames gradually moved back to an other position closer to the burner. This shift prevents the flame from moving too far away and reduces the airflow speed near the combustor entrance. Moreover, this increase in O_2 molar concentration facilitated the transition to combustion kinetics, leading to a wider and volumetrically distributed flame within the combustion chamber.
The contour representations in the combustion chamber are related to the scale of the system. However, the color distributions and temperature variations observed in these contour maps can offer insights into the transition towards homogeneity within the combustion chamber, as well as the dispersion of the flame. In combustion systems, the analysis of temperature and species distribution is crucial for understanding the combustion dynamics, flame behavior, and overall system efficiency. The color contours often depict gradients of temperature, with warmer regions typically shown in warmer colors (e.g., red, orange), and cooler regions in cooler colors (e.g., blue, green). By analyzing these patterns, one can observe how the combustion process evolves from areas of high-temperature intensity (typically near the flame front) to areas of lower temperature that are less affected by combustion processes. The transition to homogeneity refers to the tendency of the combustion products and the combustion environment to approach a more uniform distribution in terms of temperature, pressure, and species concentrations over time or after a certain period of operation. This homogeneity is an important indicator of the stability and efficiency of the combustion process. The flame's dispersion, on the other hand, refers to the spread or diffusion of the flame front within the combustion chamber, which may change due to variations in fuel supply, air-fuel mixing, or turbulence [26–28].

NO_X Pollutants emission

The final part of the study investigated the effects of hydrogen and oxygen addition on NO_X emissions at the combustion chamber exit. NO_X emissions occur through various mechanisms. The most dominant is the thermal NO_X mechanism, which occurs via high flame temperatures. Furthermore, NO_X emissions also happen due to nitrogen atoms in the fuel. Other NO_X formation pathways are the Prompt NO_X and NNH mechanisms [29]. The hydrogen and oxygen gases used in addition to methane in this study are known to increase the adiabatic flame temperature. The increase in adiabatic flame temperature triggers thermal NO_X emissions. While oxygen and hydrogen additions increase the reaction's heat, they also provide advantages and affect NO_X emissions. Therefore, examining NO_X emissions is of great importance for this study. Figure 8 shows the effect of oxygen enrichment at different H_2 ratios on the axial distribution of NO_X emissions within the boiler. In their experimental studies, Zhang et al. [30] showed the NOx emission value as approximately 7 ppm for 100% methane fuel combustion. Similarly, Kumuk [31] measured the NOx pollutant emission value as 8 ppm due to pure methane combustion in a similar combustion chamber. When the literature review is done, it is seen that the results are approximately compatible. When the graphs are examined, it can be seen that NO_X emissions increase at all hydrogen addition rates. However, there was no significant increase in NOX emissions at 30% hydrogen under standard air combustion conditions. On the other hand, oxygen-enriched combustion resulted in higher NO_X emissions. As the O_2 ratio increased, there was a significant increase in NO_X emissions. It is also clear that NO_X emissions vary linearly with flame temperature. NO_X emissions also decreased at 33.9% O_2, where the flame temperature decreased again. This is an expected result due to the thermal NO_X mechanism. When both combustion chamber temperatures and NO_X emissions are considered together, burning a fuel mixture containing 30% H_2 by volume at 26.1% O_2 appears to be the most optimal result. In this case, hydrogen energy and the O_2 gas produced by electrolysis can be an alternative fuel. Furthermore, NO_X emissions remain below 10 ppm. Figure 9 also shows the predicted NO_X contours within the combustion chamber. Thus, it can be concluded that NO_X distributions are nearly uniform throughout the combustion chamber, proving that a distributed regime is achieved for all fuels used.

4. Conclusions

This study proposes using the hydrogen gas produced by electrolysis directly in a natural gas burner rather than storing it. The use of oxygen released simultaneously with hydrogen for enrichment was also analyzed. Unlike the literature, this study used an industrial burner instead of pilot burners. The study results are as follows:

- The increased volumetric H_2 content in the fuel mixture increased the combustion chamber exit temperature due to its lower heating value.
- Oxygen-enriched combustion increased flame and combustion chamber exit temperatures up to 31% O_2. After this rate, instabilities were triggered due to the increased flame speed, leading to a decrease in flame temperature.
- An examination of the combustion chamber's axial temperature distribution revealed that while high O_2 concentrations exhibit sudden combustion and high temperatures at the burner exit, the temperature drops rapidly as the burner reaches a distance of 0.3 meters.
- NO_X emissions vary in direct correlation with combustion chamber exit temperatures. While H_2 and O_2 additions increase NO_X emissions, a 33.9% decrease in NO_X emissions was observed, decreasing both flame and combustion chamber exit temperatures.
- Considering temperature and NO_X emissions, the optimal combustion temperature was a mixture containing 70% CH_4 and 30% H_2, combined with air containing 26.1% O_2.

Acknowledgments

In this study, one of the authors, Osman KUMUK, was supported by the COST Action CA22151 STSM project. Buğrahan Alabaş was supported by the Scientific and Technological Research Council of Turkey (TÜBİTAK - 2219).

Authors' Credit

-Osman Kumuk : Conceptualization; Investigation; Software; Validation; Original draft; Writing – review & editing
-Isabel Amez :Investigation; Supervision; Validation; Original draft; Writing – review & editing
-Bugrahan Alabas:Conceptualization; Investigation; Software; Validation; Original draft; Writing – review & editing

Funding

This research did not receive any specific grant from funding agencies in the public, commercial, or not-for-profit sectors.

Conflicts of interest

The authors declare that they have no known competing financial interests or personal relationships that could have appeared to influence the work reported in this paper.

References

1. Cengel, Y. A. and Boles, M. A., Thermodynamics : An Engineering Approach, 8th Edn., McGraw-Hill Education, pp. 1-992 (2014).
2. Shiva Kumar, S. and Himabindu, V., "Hydrogen production by PEM water electrolysis – A review", *Materials Science for Energy Technologies*, **2**(3), pp. 442–454 (2019). https://doi.org/10.1016/j.mset.2019.03.002
3. El-Shafie, M., "Hydrogen production by water electrolysis technologies: A review", *Results in Engineering*, **20**, p. 101426 (2023). https://doi.org/10.1016/j.rineng.2023.101426
4. Jones, ADS. and Yen, K., Solutions: Hydrogen Use in Natural Gas Pipeline, UL solutions, pp. 1-23 (2023).
5. Amez, I., Alabas, B., Chamberlain, J., et al. "Combining hydrogen production and oxyfuel systems for energy stability and direct usage of produced oxygen. Experimental study on oxygen enriched combustion in conventional boilers", *International Journal of Hydrogen Energy*, **127**, pp. 882–895 (2025). https://doi.org/10.1016/j.ijhydene.2025.04.161
6. Al Bishtawi, B., Cheng, X., Tran, M. V., et al. "Exploration of the effects of flow parameters and hydrogen addition for methane – air laminar flame development and anchoring", *Fuel*, **403**, p. 136098 (2026). https://doi.org/10.1016/j.fuel.2025.136098
7. Alsharif, A. M. A. and Woolley, R., "Influence of equivalence ratio and hydrogen addition on thermoacoustic instabilities in premixed methane and propane flames in vertical tubes", *Case Studies in Thermal Engineering*, **69**, p. 106035 (2025). https://doi.org/10.1016/j.csite.2025.106035
8. Bayramoğlu, K., Yılmaz, S., and Bayramoğlu, T., "Effect of SMR and hydrogen-enriched methane combustion on emissions and performance", *International Journal of Hydrogen Energy*, **142**, pp. 1054–1066 (2025). https://doi.org/10.1016/j.ijhydene.2025.05.045
9. Zhao, X., Cheng, L., Wang, B., et al. "Numerical investigation for the pollutant formation of hydrogen-methane co-combustion in a porous media burner", *International Journal of Hydrogen Energy*, **143**, pp. 441–453 (2025). https://doi.org/10.1016/j.ijhydene.2025.01.154
10. Xu, S., Dou, C., Tian, Z., et al. "Experimental and numerical study on formation and NO emission of hydrogen-enriched methane combustion in swirl flame and MILD modes", *International Journal of Hydrogen Energy*, **101**, pp. 848–862 (2025). https://doi.org/10.1016/j.ijhydene.2024.12.439
11. Wang, J., Huang, Z., Tang, C., et al. "Numerical study of the effect of hydrogen addition on methane–air mixtures combustion", *International Journal of Hydrogen Energy,* **34**(2), pp. 1084–1096 (2009). https://doi.org/10.1016/j.ijhydene.2008.11.010
12. Huang, Z., Zhang, Y., Zeng, K., et al. "Measurements of laminar burning velocities for natural gas–hydrogen–air mixtures", *Combustion and Flame*, **146**(1–2), pp. 302–311 (2006). https://doi.org/10.1016/j.combustflame.2006.03.003.
13. Huang, Z., "Fuel blend combustion for decarbonization", *Proceedings of the Combustion Institute*, **40**(1–4), p. 105776 (2024). https://doi.org/10.1016/j.proci.2024.105776
14. Alabas, B. and Kumuk, O., "An experimental study on CH4–H2–NH3 fuel blends: flame stability and emission reduction in a combustor", *Fuel*, **414**, p. 138335 (2026). https://doi.org/10.1016/j.fuel.2026.138335
15. Guo, X., Chen, R., Huang, S., et al. "Enhanced premixed ammonia combustion by hydrogen-oxygen enriched pre-chamber jet ignition", *Journal of the Energy Institute*, **121**, p. 102164 (2025). https://doi.org/10.1016/j.joei.2025.102164
16. An, Z., Wang, R., Mao, R., et al. "Flame stability and emission characteristics of oxygen-enriched ammonia combustion in a swirl combustor", *Energy*, **324**, p. 135829 (2025). https://doi.org/10.1016/j.energy.2025.135829
17. Tunç, G., "Swirl number effects on combustion characteristics of oxygen-enriched methane-hydrogen fuel mixture under acoustic excitation conditions", *International Journal of Hydrogen Energy*, **101**, pp. 1014–1028 (2025). https://doi.org/10.1016/j.ijhydene.2025.01.012

18. Ilbas, M., Kumuk, O., and Karyeyen, S., "Modelling of the gas-turbine colorless distributed combustion: An application to hydrogen enriched – kerosene fuel", *International Journal of Hydrogen Energy*, **47**(24), pp. 12354–12364 (2022). https://doi.org/10.1016/j.ijhydene.2021.06.228
19. "Ansys Incorporated. Fluent 18.0, User's Guide, 2017." (n.d.).
20. Spalding, D. B., "Mixing and chemical reaction in steady confined turbulent flames", *Symposium (International) on Combustion*, **13**(1), pp. 649–657 (1971). https://doi.org/10.1016/s0082-0784(71)80067-X
21. M. Ilbas, Doctorate Thesis: Studies of ultra low NOX burner, University of Wales, College of Cardiff, UK (1997).
22. Ma, P., Deng, H., Wen, X., et al. "Studies on properties of laminar premixed oxygen-enriched NH3/H2/O2/N2 flames at elevated temperature and pressure", *Journal of the Energy Institute*, **114**, p. 101645 (2024). https://doi.org/10.1016/j.joei.2024.101645
23. Cai, X., Wang, J., Zhang, W., et al. "Effects of oxygen enrichment on laminar burning velocities and Markstein lengths of CH4/O2/N2 flames at elevated pressures", *Fuel*, **184**, pp. 466–473 (2016). https://doi.org/10.1016/j.fuel.2016.07.011
24. Min, J., Baillot, F., Guo, H., et al. "Impact of CO2, N2 or Ar diluted in air on the length and lifting behavior of a laminar diffusion flame", *Proceedings of the Combustion Institute*, **33**(1), pp. 1071–1078 (2011). https://doi.org/10.1016/j.proci.2010.06.100
25. Alabaş, B., Yılmaz, İ., and Çam, Y., "N2 and Ar dilution on the premixed biogas jet flame under external acoustic enforcement", *Propulsion and Power Research*, **12**(4), pp. 486–504 (2023). https://doi.org/10.1016/j.jppr.2023.09.001
26. Kumuk, O., "Effect of colorless distributed combustion technique on temperature and emission of hydrogen-rich coke oven gases", *International Journal of Hydrogen Energy*, **143**, pp. 978-988 (2024). https://doi.org/10.1016/j.ijhydene.2024.12.241
27. Alabas, B., Kumuk, O. and Ozcan A. "Investigation of the effect of colorless distributed combustion method on the flame of methane/hydrogen fuel mixture using image processing method", *International Journal of Hydrogen Energy*, **116**, p. 312-322 (2025). https://doi.org/10.1016/j.ijhydene.2025.03.026
28. Kumuk, B., "Performance analysis of a combustor-solid oxide fuel cell system under colorless distributed combustion conditions", *International Journal of Hydrogen Energy,* **142**, pp. 906–917 (2025). https://doi.org/10.1016/j.ijhydene.2025.01.357
29. Blaszczak RJ., Nitrogen Oxides (NOx): Why and How They Are Controlled. .S. Environmental Protection Agency, Clean Air Technology Center, pp. 1-57 (1999).
30. Zhang, H., Yao, B., Zhang, H., et al. "Synergistic effects of dilution gases and hydrogen on methane/air laminar combustion characteristics and NOX-emission concentrations", *International Journal of Hydrogen Energy*, **88**, pp. 779–791 (2024). https://doi.org/10.1016/j.ijhydene.2024.09.216
31. Kumuk, O., "Colorless distributed combustion effects on hydrogen-enriched methane fuels combustion in a laboratory-scale combustor", *Fuel*, **381**, p. 133590 (2025). https://doi.org/10.1016/j.fuel.2024.133590

Biographies

Osman KUMUK is an Assistant Professor at Iskenderun Technical University. His fields of study are: Gas turbine combustors, aeronautical engineering, numerical combustion, experimental combustion. He has many papers about combustion in international journals.

Isabel AMEZ ARENILLAS is an Associate Professor at Universidad Politecnica de Madrid. Her fields of study are: Gas turbine combustors, numerical combustion, experimental combustion, biofuel production, hydrogen production and storage, flammability. She has many papers about combustion in international journals.

Bugrahan ALABAS is an Associate Professor at Erciyes University. His fields of study are: Gas turbine combustors, aeronautical engineering, numerical combustion, experimental combustion, aerodynamics, supersonics flows. He has many papers about combustion in international journals.

Figure and table captions

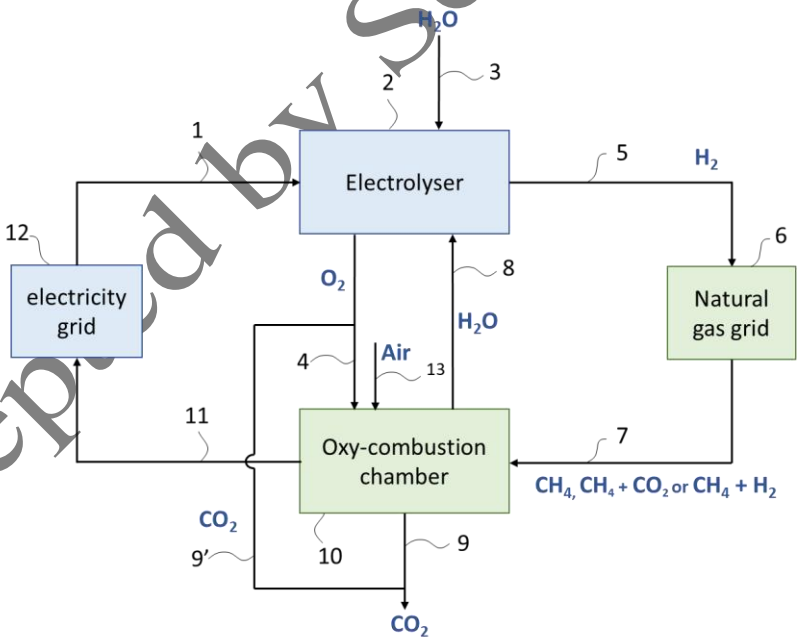

Figure 1

Table 1

Definition	Value/Parameter	Unit
Inlet Turbulent Intensity	8	%
Thermal Power	33	kW
Equivalence Ratio	0.83	---
Convective heat transfer coefficient	30	W/m2.K
Wall Thickness of the Combustor	0.002	m
Solver	Pressure-Based	---
Spatial Discretization	Second Order Upwind	---
Gradient	Least Squares Cell Based	---
Pressure	Presto	---
Mesh Nodes	338269	---
Mesh Elements	318768	

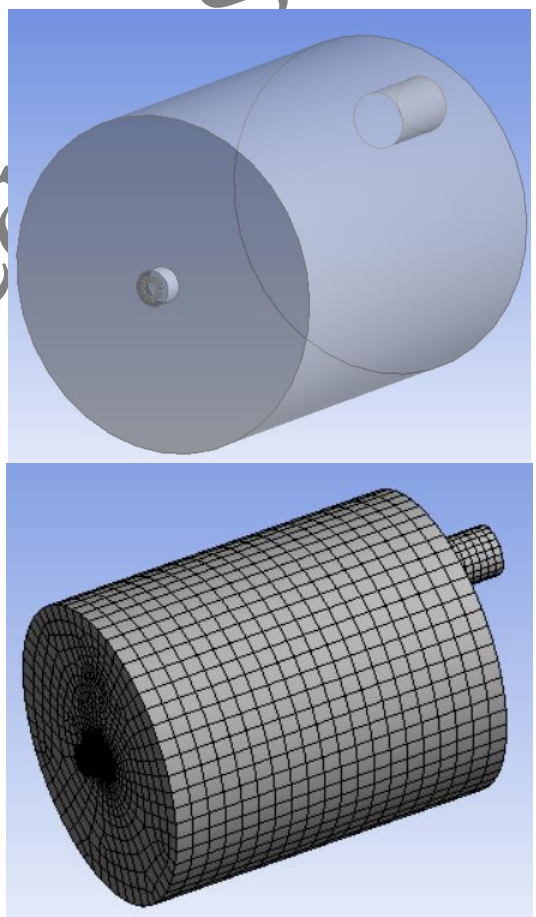

Figure 2

Table 2

Mixtures	NG Flow Rate (sccm)	H_2 Flow Rate (sccm)	O_2 / N_2 + O_2 (Volumetric)	LHV (kJ/kg)
%100 NG	55071	0	20.8, 23.5, 26.1, 28.5, 31, 33.9	50144
%90 NG - %10 H_2	53270	5919	20.8, 23.5, 26.1, 28.5, 31, 33.9	51114
%80 NG - %20 H_2	51181	12795	20.8, 23.5, 26.1, 28.5, 31, 33.9	52289
%70 NG - %30 H_2	48726	20883	20.8, 23.5, 26.1, 28.5, 31, 33.9	53743

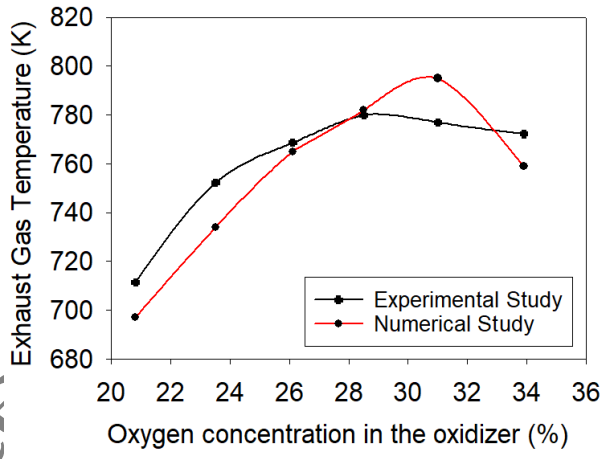

Figure 3

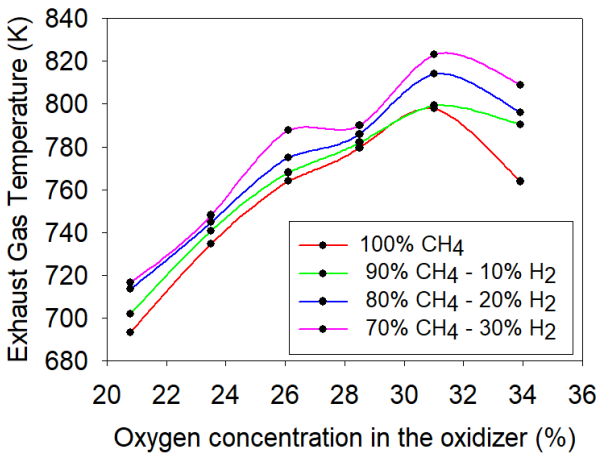

Figure 4

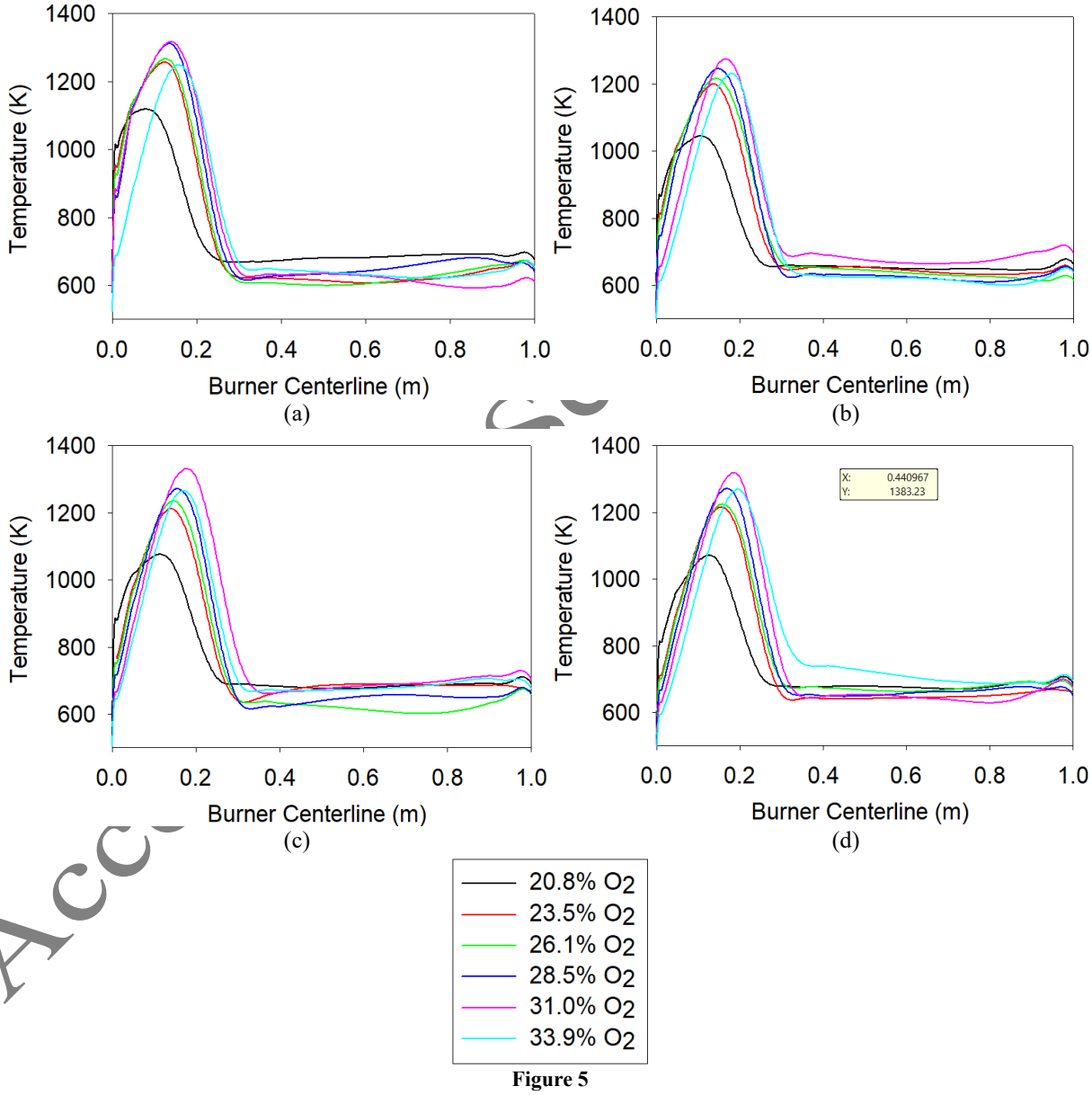

Figure 5

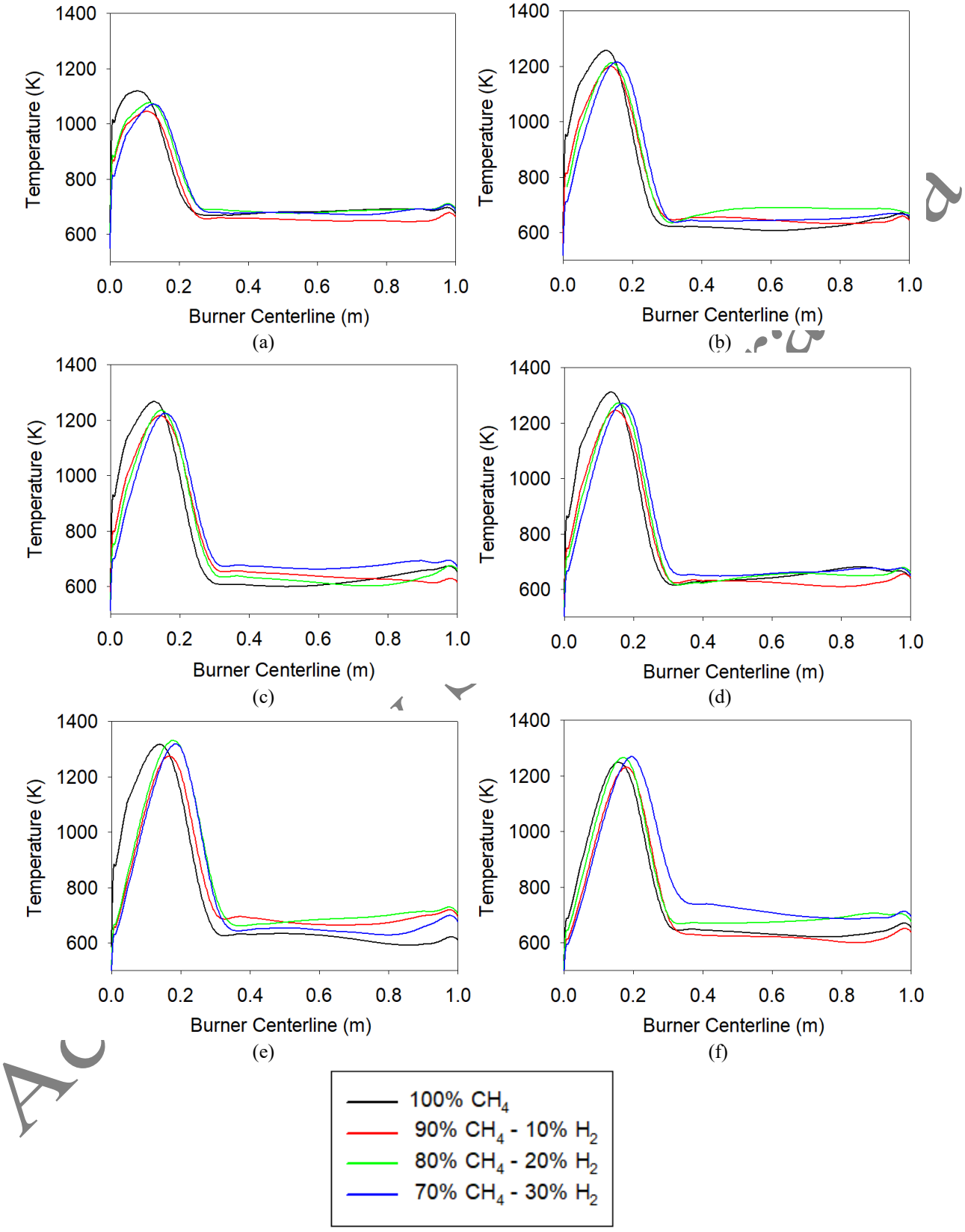
Temperature (K)
Burner Centerline (m)
(a)
(b)
(c)
(d)
(e)
(f)
100% CH4
90% CH4 - 10% H2
80% CH4 - 20% H2
70% CH4 - 30% H2

Figure 6

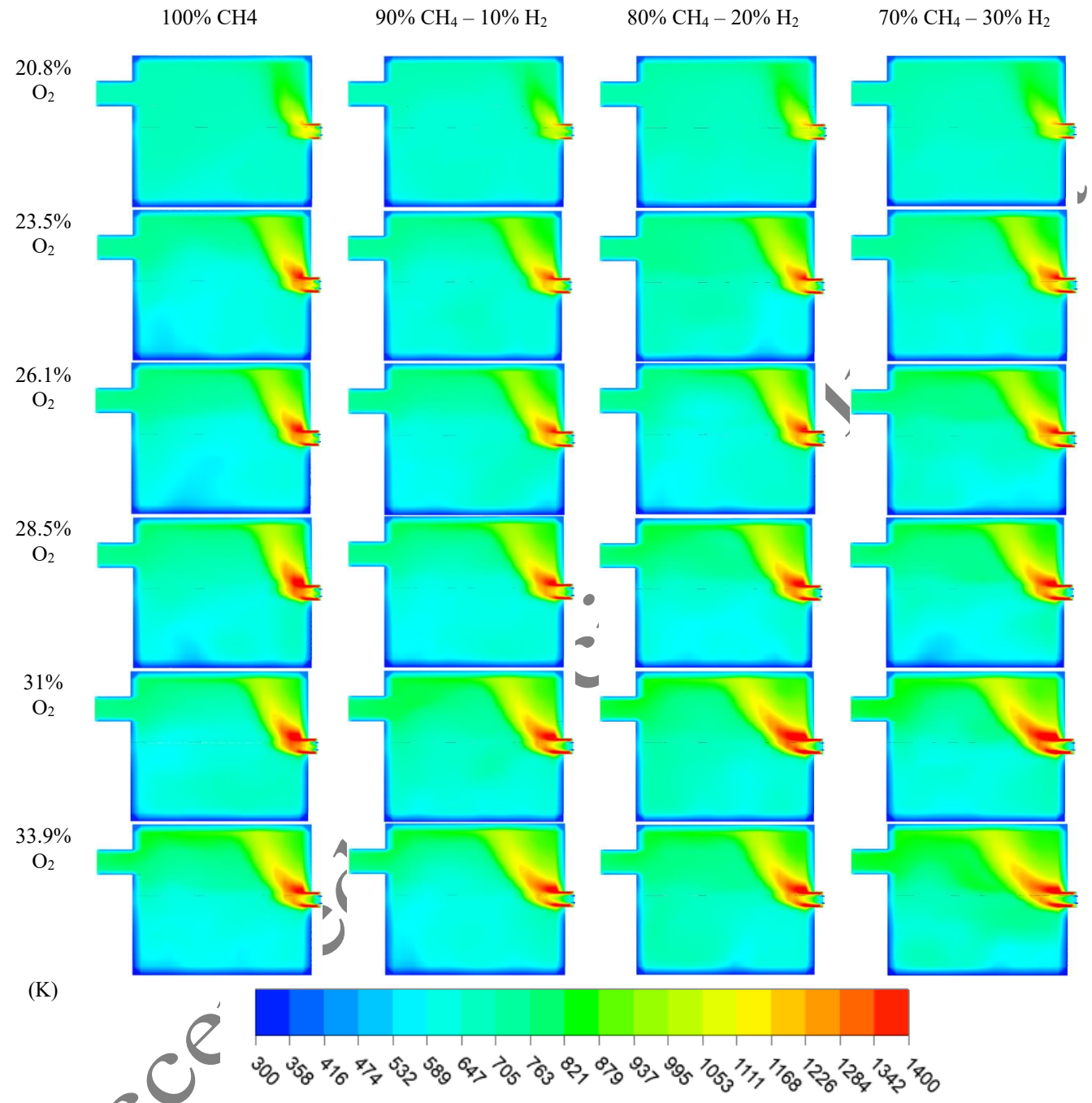

Figure 7

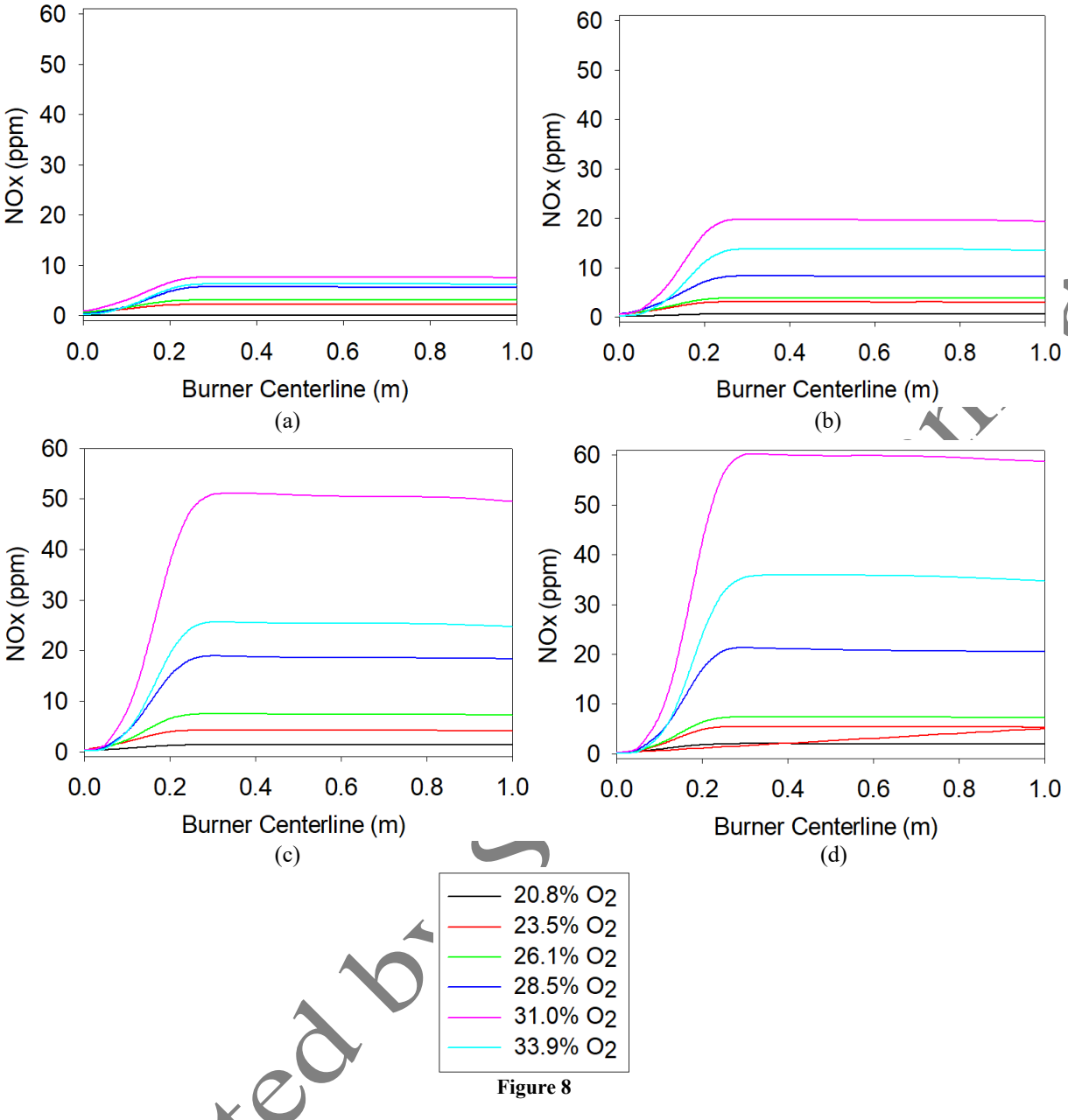

Figure 8

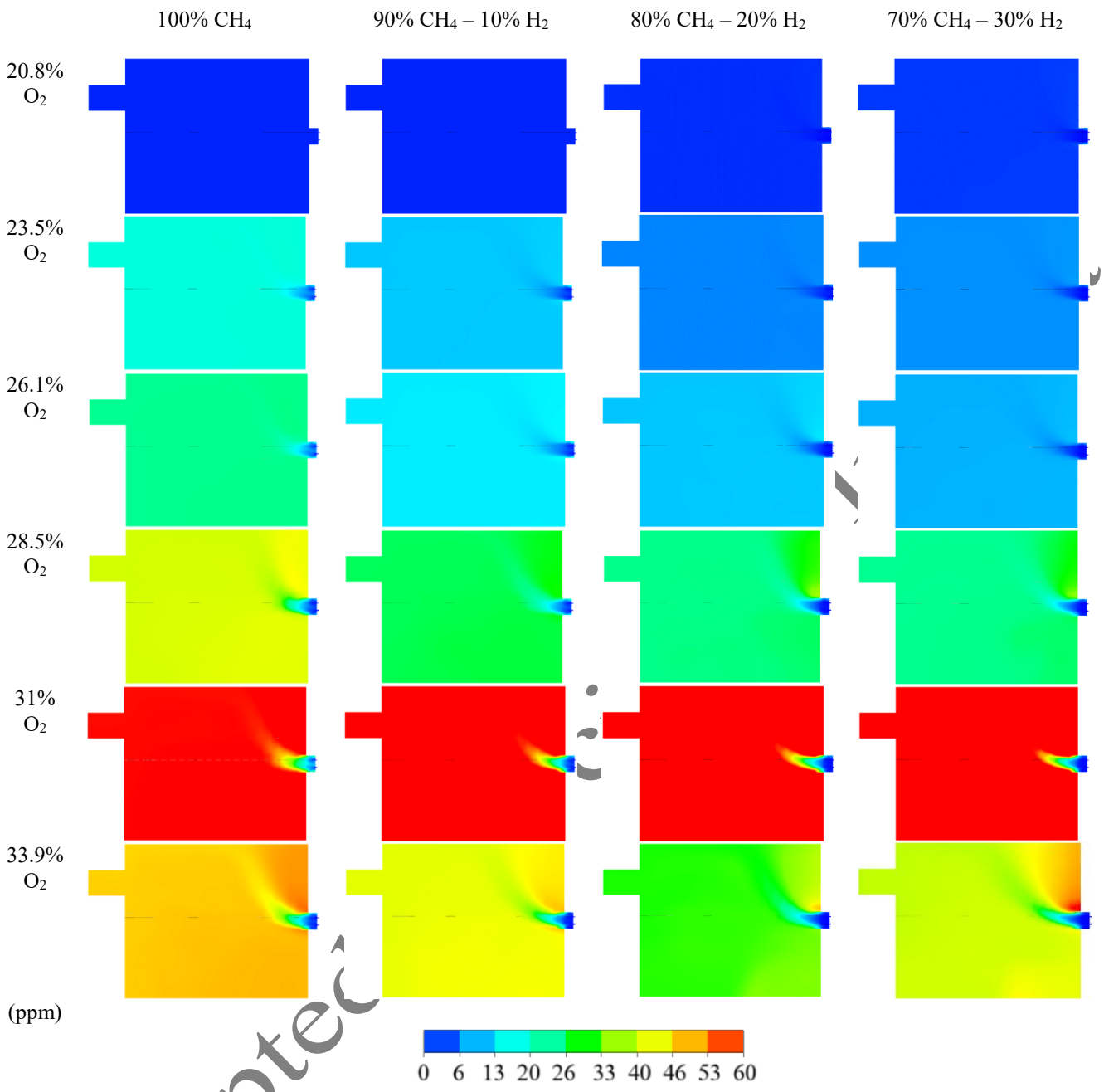

Figure 9